

Single-cell detection of microRNAs in developing vertebrate embryos after acute administration of a dual-fluorescence reporter/sensor plasmid

Davide De Pietri Tonelli¹, Federico Calegari¹, Ji-Feng Fei¹, Tadashi Nomura², Noriko Osumi², Carl-Philipp Heisenberg¹, and Wieland B. Huttner¹

¹Max Planck Institute of Molecular Cell Biology and Genetics, Dresden, Germany and

²Tohoku University Graduate School of Medicine, Sendai, Japan

BioTechniques 41:727-732 (December 2006)

doi 10.2144/000112296

The detection of microRNAs (miRNAs) at single-cell resolution is important for studying the role of these posttranscriptional regulators. Here, we use a dual-fluorescent green fluorescent protein (GFP)-reporter/monomeric red fluorescent protein (mRFP)-sensor (DFRS) plasmid, injected into zebrafish blastomeres or electroporated into defined tissues of mouse embryos in utero or ex utero, to monitor the dynamics of specific miRNAs in individual live cells. This approach reveals, for example, that in the developing mouse central nervous system, miR-124a is expressed not only in postmitotic neurons but also in neuronal progenitor cells. Collectively, our results demonstrate that acute administration of DFRS plasmids offers an alternative to previous in situ hybridization and transgenic approaches and allows the monitoring of miRNA appearance and disappearance in defined cell lineages during vertebrate development.

INTRODUCTION

MicroRNAs (miRNAs) are 20–25 nucleotide long noncoding RNAs that have been found in a wide variety of organisms and shown to exert essential roles by regulating the stability and translation of target messenger RNAs (mRNAs) (1–4). Interestingly, most miRNAs show tissue-specific and developmentally regulated expression (5–8). To investigate the role played by miRNAs during development, the establishment of techniques allowing the detection/monitoring of miRNA expression during cell fate change in vivo is crucial (9). To detect miRNAs in tissues microscopically, two ingenious approaches have been used: (i) in situ hybridization using locked nucleic acid (LNA)-modified DNA oligonucleotide probes, which detect the presence of miRNAs irrespective of their potential activity (8) and (ii) the expression or administration of target mRNAs (sensors), which detect miRNAs via

their degradation-triggering activity toward the sensor (10–12).

Although both approaches are powerful, certain limitations remain. Thus, in situ hybridization using LNA probes requires tissue fixation, which prevents the monitoring of miRNA appearance/disappearance in a given cell lineage during cell fate change. While this limitation could potentially be overcome by in vivo expression of a sensor mRNA encoding a fluorescent protein, the latter approach has typically involved the generation of transgenic animals (10,11). Moreover, in the sensor approach, a lack of signal is interpreted as being indicative of the presence of a miRNA, which calls for some means of verification that the sensor mRNA is actually being transcribed in the cell lacking sensor protein. Overcoming these limitations, we report here a relatively simple and reliable system that allows the detection of miRNAs with cellular resolution in vivo without the need to generate transgenic animals.

MATERIALS AND METHODS

DFRS Plasmids

Details concerning the construction of the dual-fluorescent green fluorescent protein (GFP)-reporter/monomeric red fluorescent protein (mRFP)-sensor (DFRS) plasmids used are provided in the supplementary materials available online at www.BioTechniques.com.

Zebrafish Embryo Injection

All embryos were obtained from the zebrafish AB wild-type line. Single blastomeres of 2- to 8-cell stage embryos were injected with approximately 500 pL phosphate-buffered saline (PBS) containing, as the standard concentration, 0.1 µg/µL purified DFRS plasmid. In some experiments, a higher concentration (0.5 µg/µL) was used. Embryos were maintained in E3 medium and manipulated by standard methods (13).

Mouse Embryo Electroporation

In utero electroporation of mouse embryos was performed as described (14), except that the topology of the embryos was determined using illumination and a dissecting microscope rather than ultrasound microscopy. Pregnant mice 13 days postcoitum were anesthetized with isoflurane vapor and their uteri exposed. Using a glass capillary, 1–3 µL PBS containing 3–5 µg/µL DFRS plasmid were injected through the uterine wall into the lumen of the telencephalic vesicles or released in proximity of the ectoderm of the embryo. Immediately after injection, 6 square electrical pulses of 30 V, 50 ms each at 1-s intervals were delivered through platinum electrodes (2 mm diameter) using a BTX®-ECM®830 electroporator (Harvard Apparatus, Holliston, MA, USA). The orientation of the electric field was used to direct the uptake of the plasmid to specific regions of the developing brain or ectoderm. After electroporation, the uterus was relocated into the peritoneal cavity, and the abdomen was sutured. Mice were sacrificed either 24 or 72

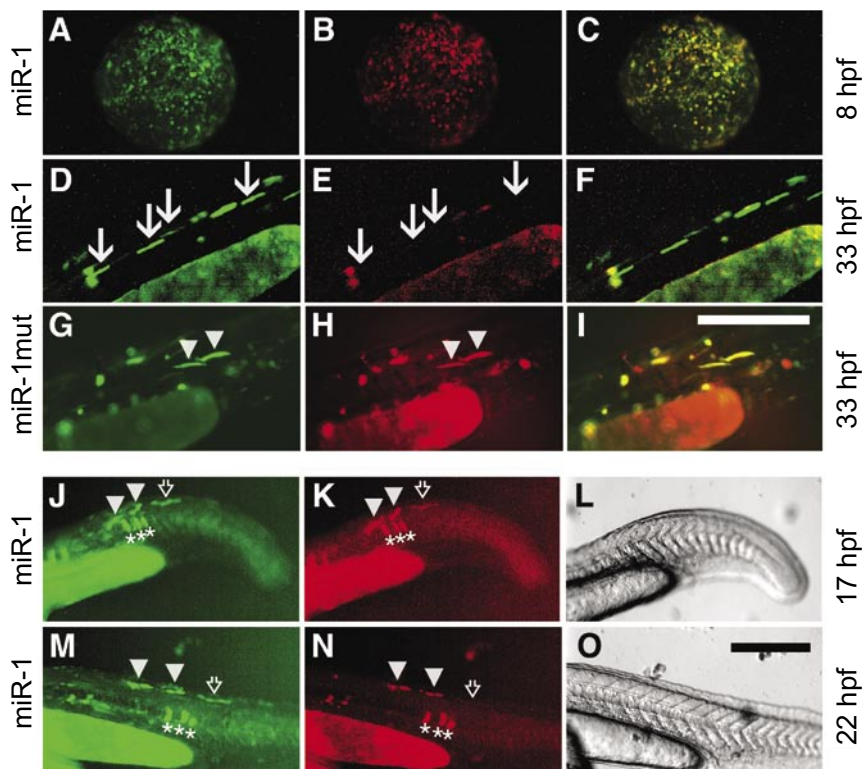


Figure 1. In vivo visualization of miR-1 dynamics during skeletal muscle development in zebrafish. Dual-fluorescent green fluorescent protein (GFP)-reporter/monomeric red fluorescent protein (mRFP)-sensor (DFRS) miR-1 plasmid (A–F and J–O) or mutated DFRS miR-1 plasmid (G–I) was injected into single blastomere of 2- to 4-cell stage (A–I) or 8-cell stage (J–O) zebrafish embryos, followed by analysis of GFP (A, D, G, J, M) and mRFP (B, E, H, K, N) fluorescence in cells after 8 h (A–C), 17 h (J–L), 22 h (M–O), and 33 h (D–I) postfertilization (hpf); merge (C, F, I). Note that (J–L) and (M–O) are the same embryo 5 h apart; (L and O) bright field. Triangles indicate muscle fibers containing both GFP-reporter and mRFP-sensor. Arrows in (D and E) indicate muscle fibers showing GFP-reporter but no longer mRFP-sensor fluorescence. Open arrows in (J, K, M, N) indicate a muscle fiber that shows both GFP-reporter and mRFP-sensor fluorescence 17 hpf (J and K), but has lost the mRFP fluorescence 5 h later (N). Asterisks in (J, K, M, N) indicate notochord cells that maintain both green and red fluorescence. Fluorescent dots in panels M and N that are outside of the embryo presumably are autofluorescent methylcellulose crystals in the mounting medium used for live imaging. (D–O) Orientation of embryos: caudal, right; ventral, down. Scale bars, 250 μ m; A–I and J–O, respectively, are the same magnification.

h after in utero electroporation, and the embryos were collected for further analyses. Ex utero electroporation of DFRS plasmids into telencephalic vesicles of E10 mouse embryos followed by 24 h of whole-embryo culture was performed as described previously (15).

In Situ Hybridization on Cryosections Using LNA-Modified Oligonucleotides

Whole-mount E11 and E14 mouse embryos were fixed overnight at 4°C in 4% paraformaldehyde in 120 mM phosphate buffer, pH 7.4, equilibrated in 30% sucrose in PBS, and embedded in Tissue-Tek®, and 10- μ m cryosections were prepared. In situ hybrid-

ization was performed according to standard protocols with the following modifications. LNA-modified DNA oligonucleotides (Exiqon A/S, Vedbaek, Denmark) were labeled with digoxigenin (DIG)-ddUTP using the DIG oligonucleotide 3' end labeling kit (Roche Diagnostic GmbH, Mannheim, Germany) according to manufacturer's instructions. Prehybridized cryosections were incubated overnight at 51°C (miR-9) or 59°C (miR-124a) in hybridization buffer containing 200 pmol/mL of DIG-labeled LNA-oligonucleotide. Following incubation with alkaline phosphatase-conjugated anti-DIG antibody at 4°C overnight, staining with 5-bromo-4-chloro-3-indoxyl phosphate/nitro blue tetrazolium (BCIP/NBT; Sigma-Aldrich Chemie

GmbH, Taufkirchen, Germany) was done at 37°C for 2 h and then either at 4°C for 1–2 days or at room temperature for 6–12 h. Images were acquired with a standard upright microscope (Olympus® Optical, Europe GmbH, Hamburg, Germany).

Fluorescence Microscopy

Anesthetized zebrafish, at the indicated stages of development, and whole-mount mouse embryos or dissected brains (unfixed) were imaged using a Model SZX12 dissecting microscope equipped with epifluorescence (Olympus, Hamburg, Germany). Cryosections of brains, fixed as above, were permeabilized with 0.3% Triton® X-100 in PBS and quenched with 10 mM NH₄Cl prior to analysis using a Model BX61 fluorescence microscope (Olympus) or an Axiovert 200 laser-scanning confocal microscope (Carl Zeiss GmbH, Jena, Germany). Images were acquired and processed using the IPlab software version 3.5.1 (Scanalytics, Rockville, MD, USA) or the Zeiss LSM Image Examiner software version 3.2.0.70 (Carl Zeiss GmbH).

RESULTS AND DISCUSSION

Dual-Fluorescence GFP-Reporter/ mRFP-Sensor Plasmid

Our system is based on the acute administration of a DFRS plasmid for a specific miRNA into the organism of interest. In our DFRS plasmids, both GFP and mRFP are under the control of identical constitutive promoters [Supplementary Figure S1, simian virus 40 (SV40)]. The GFP-reporter was used to identify the cells actually expressing the plasmid, given that the sensor-based strategy relies on the silencing of a transcript. The mRFP-sensor contained a 3' untranslated region (UTR) with a tandem cassette (10,11) complementary to the miRNA of interest (Supplementary Figure S1). Two types of DFRS control plasmids were used. First, for each miRNA-complementary sequence, three nucleotides in the region complementary to the “seed” of the miRNA of interest were mutated

(Supplementary Figure S1, referred to as mutated DFERS plasmid). Second, we used a DFERS plasmid that contained a tandem cassette with an arbitrary sequence that was not complementary to any known miRNA (Supplementary Figure S1, referred to as DFERS control plasmid).

Visualization of miR-1 Appearance in Skeletal Muscle Fibers of Developing Zebrafish Using a DFERS Plasmid

We initially explored the use of DFERS plasmids for miRNA detection using the zebrafish as a model system. Specifically, we tested a DFERS plasmid for miR-1, which has been shown to be expressed in developing skeletal muscle of zebrafish (8). The DFERS miR-1 plasmid was injected into one blastomere of 2- to 8-cell stage embryos, and embryos were allowed to develop for up to 9 days, resulting in

mosaic transgene expression. After 8 hours postfertilization (hpf) (approximately 75%–80% of epiboly; i.e., before the onset of skeletal muscle development) (16), both GFP-reporter and mRFP-sensor fluorescence were observed, being colocalized in most, if not all, cells (Figure 1, A–C). This indicated that miR-1 was not yet expressed at this early stage of zebrafish development. At a later stage (i.e., after 33 hpf) when skeletal muscle has been formed (16), most of the GFP-expressing fibers did not show mRFP-sensor fluorescence (Figure 1, D–F, arrows); these were identified as muscle fibers by whole-mount immunostaining 72 hpf using an anti-myosin heavy chain antibody (Supplementary Figure S2). After 9 days postfertilization (dpf), essentially all GFP-expressing muscle fibers lacked mRFP-sensor fluorescence (Supplementary Figure S3). In contrast to the results obtained with the DFERS miR-1 plasmid, both

GFP-reporter and mRFP-sensor fluorescence were observed in muscle fibers after blastomere injection of the mutated DFERS miR-1 plasmid 33 hpf (Figure 1, G–I, triangles) and of the DFERS control plasmid 33 hpf (not shown) and 9 dpf (Supplementary Figure S3). We therefore conclude that the lack of mRFP-sensor fluorescence in DFERS miR-1 plasmid-expressing muscle fibers at 33 hpf and thereafter indicated the presence of active miR-1, (which prevented further synthesis of mRFP), consistent with previous microarray and *in situ* hybridization data (8). On a more general note, our observations demonstrate that the use of a DFERS plasmid, by allowing the comparison between GFP-reporter and mRFP-sensor fluorescence, provides certainty in interpreting the lack of sensor fluorescence as being indicative of the presence of a miRNA (rather than the lack of transcription of the sensor gene).

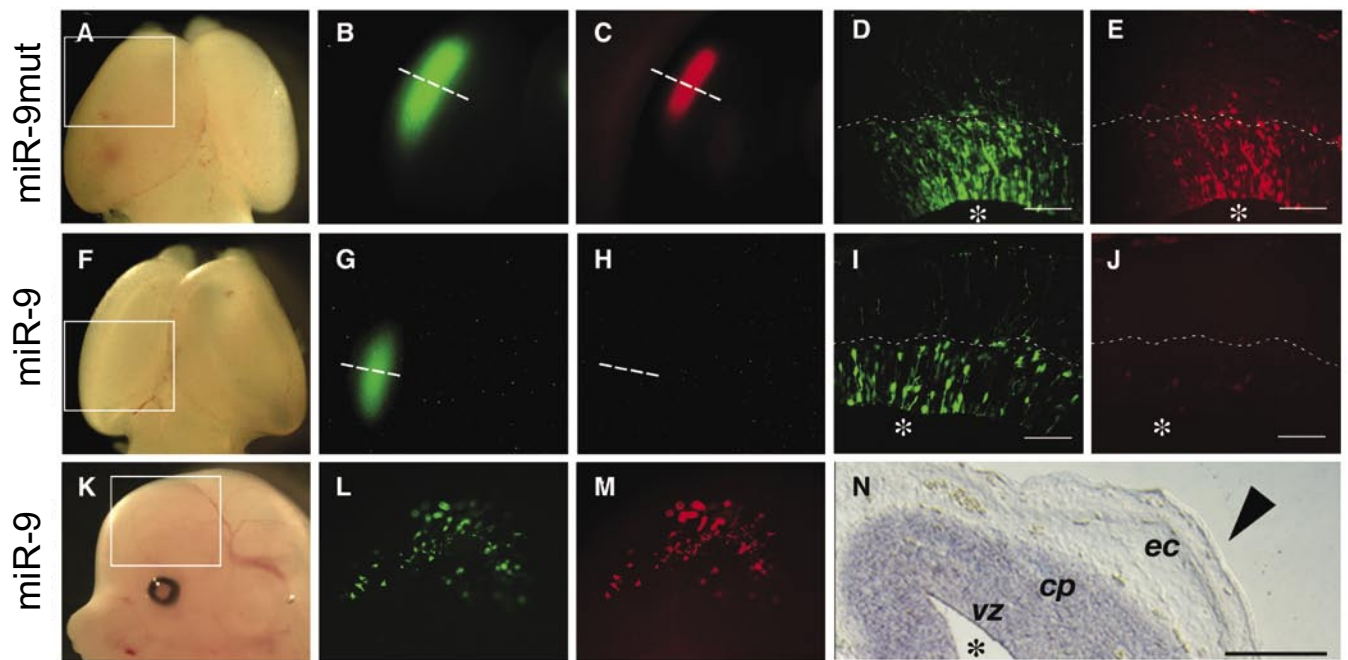


Figure 2. Single-cell detection of miR-9 in the embryonic mouse brain by *in utero* electroporation of a dual-fluorescent green fluorescent protein (GFP)-reporter/monomeric red fluorescent protein (mRFP)-sensor (DFERS) plasmid. DFERS miR-9 plasmid (F–M) or mutated DFERS miR-9 plasmid (A–E) was injected into the lumen of the telencephalic vesicles (A–J) or administered in proximity of the ectoderm (K–M) of E13 mouse embryos *in utero* followed by electroporation into the left telencephalic neuroepithelium and left cranial ectoderm, respectively. After 24 h of *in utero* development, dissected brains (A–C and F–H) or whole embryos (K–M) were analyzed in the targeted region (boxes in A, F, and K) for GFP (B, G, and L) and mRFP (C, H, and M) expression. Brains were then fixed, and cryosections of the region of the neural tube wall showing GFP expression (B and G, dashed lines) were examined for the presence of GFP-reporter (D and I) and mRFP-sensor (E and J) in individual cells. Note the absence of mRFP-sensor fluorescence in the brain (H) and neuroepithelial cells (J) electroporated with the DFERS miR-9 plasmid, in contrast to its presence in the ectoderm electroporated with the DFERS miR-9 plasmid (M) and in the brain (C) and neuroepithelial cells (E) electroporated with the mutated DFERS miR-9 plasmid. (N) *In situ* hybridization using a locked nucleic acid (LNA) probe for miR-9 on coronal cryosections of the E14 mouse head. Note the absence of miR-9 in the ectoderm (N, *ec*, arrowhead) and its presence in both the neuronal progenitors of the ventricular zone (N, *vz*) and postmitotic neurons in the cortical plate (N, *cp*) of the telencephalon. Asterisks indicate the ventricular lumen. Scale bars, 50 μ m (D, E, I, J) and 100 μ m (N).

To explore whether a DFRS plasmid can be used to reveal the appearance of a miRNA in a given cell, we compared, after blastomere injection of DFRS miR-1 plasmid, the intensity of mRFP-sensor fluorescence in the same muscle fibers at two time points during earlier stages of skeletal muscle development, 17 and 22 hpf. Remarkably, some muscle fibers showing both GFP and mRFP fluorescence at 17 hpf (Figure 1, J and K, open arrows) completely lost mRFP-sensor (Figure 1N, open arrow), but not GFP-reporter (Figure 1M, open arrow), fluorescence just 5 h later and other muscle fibers that still showed mRFP-sensor fluorescence at 22 hpf (Figure 1N, triangles) had lost it at 43 hpf (data not shown). In contrast, cells lacking miR-1 expression, such as those of the notochord (8), maintained both GFP-reporter and mRFP-sensor expression throughout (Figure 1, J, K, M, and N, asterisks and data not shown). These observations show that the DFRS miR-1 plasmid can be used to visualize the appearance of miR-1 activity in skeletal muscle during zebrafish development, which implies that the half-life of mRFP under the present conditions was sufficiently short so as not to obscure the appearance of the miRNA activity.

It could be argued that the disappearance of mRFP fluorescence from 17 to 22 hpf in some muscle fibers (Figure 1, K and N, open arrows) but not others (Figure 1, K and N, triangles) may reflect a lower copy number of DFRS miR-1 plasmid in the former than the latter muscle fibers. To address this issue, we compared GFP-reporter and mRFP-sensor fluorescence in various muscle fibers at 22 hpf after blastomere injection of a 5-fold higher DFRS miR-1 plasmid concentration (0.5 $\mu\text{g}/\mu\text{L}$) than the standard one (0.1 $\mu\text{g}/\mu\text{L}$). While with 0.5 $\mu\text{g}/\mu\text{L}$ DFRS miR-1 plasmid, muscle fibers showed, on average, an increase in GFP-reporter fluorescence (Supplementary Figure S4D) as compared with 0.1 $\mu\text{g}/\mu\text{L}$ DFRS miR-1 plasmid (Supplementary Figure S4A), we did not note an increase in mRFP-sensor fluorescence at the higher DFRS miR-1 plasmid concentration (Supplementary Figure S4, B and E). Moreover, at either DFRS miR-1 plasmid concen-

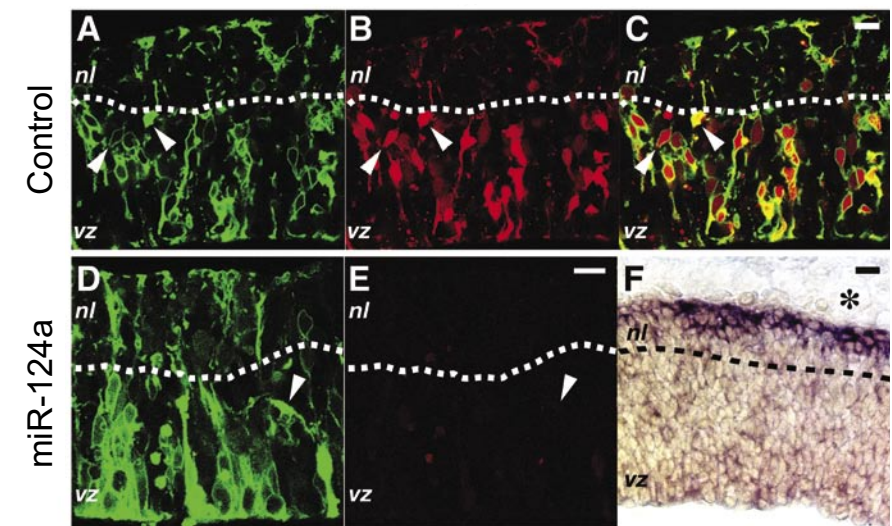


Figure 3. Acute expression of a dual-fluorescent green fluorescent protein (GFP)-reporter/monomeric red fluorescent protein (mRFP)-sensor (DFRS) plasmid in the E11 mouse brain reveals the presence of miR-124a in neuronal progenitors. (A–E) DFRS control (A–C) or miR-124a (D–E) plasmid was electroporated into the E10 mouse telencephalic neuroepithelium followed by 24 h of whole-embryo culture development, and cryosections were analyzed by confocal microscopy. Note the plasma membrane-localized GFP-reporter (A) and mRFP-sensor (B) fluorescence in neuroepithelial cells in the ventricular zone (vz) and in neurons in the ventricular zone (vz, arrowheads) and in the neuronal layer (nl) upon administration of DFRS control plasmid, but only pmGFP-reporter (D) and not mRFP-sensor (E) fluorescence in these cells upon administration of the DFRS miR-124a plasmid. (F) In situ hybridization using a locked nucleic acid (LNA) probe for miR-124a on a cryosection of E11 mouse telencephalon. Note the strong staining for miR-124a in the neuronal layer (nl) and the weak staining in the ventricular zone (vz). Dashed lines indicate the boundary between the ventricular zone and the neuronal layer. Scale bars, 10 μm .

tration, we observed muscle fibers with relatively low GFP-reporter expression (Supplementary Figure S4, A and D, arrowheads) that nonetheless showed mRFP-sensor fluorescence (Supplementary Figure S4, B and E, arrowheads), and these coexisted with muscle fibers with relatively high GFP-reporter expression (Supplementary Figure S4, A and D, arrows) that did not show mRFP-sensor fluorescence (Supplementary Figure S4, B and E, arrows). These observations indicate that the ratio of GFP-reporter/mRFP-sensor fluorescence (Supplementary Figure S4, C and F, arrowheads and arrows) did not correlate with the DFRS miR-1 plasmid expression level as revealed by GFP-reporter fluorescence, which reflects plasmid copy number (Supplementary Figure S4, A and D, arrowheads and arrows). This in turn implies that the variation in the ratio of GFP-reporter/mRFP-sensor fluorescence between individual muscle fibers at 22 hpf (Figure 1, M and N, triangles and open arrows, and Supplementary Figure S4, C and F, arrowheads and

arrows) reflected a variation in miR-1 activity, which is consistent with the development of distinct subtypes of muscle fibers (16). This issue could be investigated further by combining, similar to the approach shown in the Supplementary Figure S2, the analysis of miR-1 expression using the DFRS plasmid with immunocytochemistry using antibodies that discriminate between muscle fiber subtypes.

Single-Cell Detection of miRNAs in Mosaic Mouse Embryos after Acute Tissue Targeting of DFRS Plasmids

In contrast to zebrafish and flies, the generation of mammalian transgenic animals is much more labor-intensive. To establish a system allowing the monitoring of miRNA dynamics in defined cell lineages during mammalian embryonic development, we explored the use of DFRS plasmids in conjunction with a combination of methods previously used to achieve acute expression of transgenes and RNA interference in developing mouse

embryos. This combination consists of the topical release of nucleic acids in the proximity of a specific tissue of a mouse embryo developing either in culture or in utero and their delivery into this tissue by directed electroporation. This combination of methods has been successfully applied, in particular, to the developing mouse brain (14,15). Given that Northern blot and microarray analyses and cDNA cloning have previously shown miR-9 to be expressed in the developing and adult rodent brain (5–7,17), we explored the use of a DFRS miR-9 plasmid (Supplementary Figure S1) to detect this miRNA in the developing brain. As controls, we used (i) a DFRS miR-9 plasmid in which three nucleotides in each miR-9 complementary sequence were mutated to prevent miR-9 binding; (ii) a DFRS control plasmid, the tandem cassette of which was not complementary to any known mouse miRNA; and (iii) a DFRS plasmid that contained, instead of the tandem cassette complementary to miR-9, a tandem cassette complementary to miR-1 (Supplementary Figure S1), which is known to be expressed in the developing cardiac and skeletal muscles, but not brain, of the mouse embryo (5,11,18).

The DFRS plasmids were injected into the lumen of the telencephalic vesicles of embryonic day 13 (E13) mouse embryos in utero and electroporated into the left telencephalic neuroepithelium (Figure 2, A–J). After in utero development for 24 h, analysis of GFP-reporter and mRFP-sensor fluorescence showed that in the case of the mutated DFRS miR-9 plasmid, both fluorescent proteins were expressed in the E14 telencephalon (Figure 2, B and C), being colocalized in the same neuroepithelial cells (Figure 2, D and E). Similar results were obtained with the DFRS control plasmid or the DFRS miR-1 plasmid (data not shown), the latter finding being consistent with the lack of miR-1 expression in the developing brain (5,11,18). In contrast, in the case of the DFRS miR-9 plasmid, only GFP-reporter (Figure 2, G and I), but not mRFP-sensor (Figure 2, H and J), fluorescence was detected, indicating the presence of this miRNA in E14 telencephalic neuroepithelial cells.

To corroborate the presence of miR-9 in the neuroepithelium, we performed in situ hybridization with an LNA probe (8) on cryosections through the head of E14 mice (Figure 2N), which yield superior cellular resolution as compared with whole-mount preparations (19). Indeed, miR-9 was found to be abundantly expressed in the dorsal telencephalon of E14 mouse embryos (Figure 2N), being present in both the neuronal progenitors in the ventricular zone (Figure 2N, *vz*) (i.e., neuroepithelial cells) and the postmitotic neurons in the cortical plate (Figure 2N, *cp*), but being absent in the developing ectoderm (Figure 2N, *ec*, arrowhead). As a further control, when the DFRS miR-9 plasmid was electroporated into the E13 ectoderm (rather than brain) followed by 24 h of in utero development (Figure 2, K–M), both GFP-reporter and mRFP-sensor fluorescence were observed, being colocalized in the same cells (Figure 2, L and M). This showed that the DFRS miR-9 plasmid was functional in terms of GFP-reporter plus mRFP-sensor expression and demonstrated the absence of miR-9 in the E14 ectoderm, consistent with the results of in situ hybridization (Figure 2N, *ec*, arrowhead).

In another set of experiments, the DFRS miR-9 plasmid was electroporated into the E13 mouse diencephalic neuroepithelium followed by 3 days of in utero development. In this case, we detected GFP-reporter, but not mRFP-sensor, fluorescence not only in neuroepithelial cells but also in cortical neurons (Supplementary Figure S5), consistent with the presence of miR-9 in cortical neurons (Figure 2N, *cp*).

miR-124a Is Expressed in Neurons and Neuronal Progenitors

We extended the DFRS approach to another miRNA, miR-124a, which is thought to be expressed specifically in neurons (20). During the development of the mouse central nervous system, newborn neurons prior to their migration to the neuronal layers coexist with the neuronal progenitors in the ventricular zone. We therefore modified the DFRS plasmid by adding a plasma membrane localization signal to the GFP-reporter (pmGFP; see the

supplementary materials for details) in order to distinguish newborn neurons in the ventricular zone from neuroepithelial cells by outlining the distinct shape of these cell types. Indeed, when the DFRS control plasmid was electroporated into the E10 mouse telencephalic neuroepithelium ex utero followed by 24 h of whole-embryo culture, both the neuroepithelial cells in the ventricular zone (Figure 3, A–C, *vz*) and the neurons born in the ventricular zone (identified by the nonradial orientation of their cell body; Figure 3, A–C, *vz*, arrowheads) and present in the neuronal layer (Figure 3, A–C, *nl*) showed pmGFP-reporter and mRFP-sensor expression. Surprisingly, however, upon electroporation of the DFRS miR-124a plasmid, essentially all cells [i.e., not only the neurons born in the ventricular zone (Figure 3E, *vz*, arrowhead) and present in the neuronal layer (Figure 3E, *nl*), but also the neuroepithelial cells (Figure 3E, *vz*), which constitute the vast majority of the cells in the ventricular zone] lacked mRFP-sensor fluorescence, although there was robust expression of the DFRS miR-124a plasmid in these cells as revealed by pmGFP-reporter fluorescence (Figure 3D). The same results were obtained upon electroporation of the DFRS miR-124a plasmid into the E13 mouse telencephalic neuroepithelium followed by 24 h of in utero development, and mutation of three nucleotides of each miR-124a target sequence (Supplementary Figure S1) was sufficient to prevent mRFP-sensor silencing (data not shown). These observations indicate that, contrary to the prevailing notion (20), miR-124a is expressed not only in postmitotic neurons but also in their progenitors, the neuroepithelial cells. These unexpected results on miR-124a were corroborated by in situ hybridization with a miR-124a LNA probe (8) on cryosections of E11 mouse brain, which confirmed the presence of a low level of miR-124a in the ventricular zone (Figure 3F, *vz*) (in addition to the known massive expression in the neuronal layer; Figure 3F, *nl*). The low-level in situ hybridization signal in the ventricular zone was specific as no such signal was detected in the ectoderm (Figure 3F, asterisk), which is known to

lack miR-124a expression. Thus, on a more general note, our findings demonstrate that the acute administration of a DFRS plasmid is a valid approach to gain novel information about the expression of a given miRNA.

In conclusion, the present experimental approach of acutely administering a DFRS plasmid for a specific miRNA offers a convenient method to detect these important posttranscriptional regulators with single-cell resolution and to monitor their dynamics *in vivo*. Our approach, which presumably is applicable to a wide variety of species (including those for which transgenic lines have not been established), circumvents the need to generate transgenic organisms, which is much more labor-intensive for mice (11) than for flies (10). Moreover, the topical administration of DFRS plasmids, followed by their directed electroporation (15,21), provides a simple approach to study a specific miRNA in the tissue and cell lineage of interest.

ACKNOWLEDGMENTS

D.D.P.T. and F.C. contributed equally to this work. We thank Dr. Yoichi Kosodo for his help in establishing the in utero electroporation; Dr. Irinka Castanon, Christiane Haffner, and Sylvia Schneider for help with the experiments; Drs. Véronique Dubreuil and Christian Eckmann for advice; and Dr. Antonio J. Giraldez for helpful discussions. F.C. and W.B.H. were supported by the Federal Ministry of Education and Research (BMBF) in the framework of the National Genome Research Network, SMP RNAi, Förderkennzeichen 5 (NGFN-2). W.B.H. was supported by grants from the DFG (SPP 1109, Hu 25/7-3; SPP 1111, Hu 275/8-3; SFB/TR 13, B1; SFB 655, A2) and the Fonds der Chemischen Industrie.

COMPETING INTERESTS STATEMENT

The authors declare that the DFRS plasmid-based approach to detect miRNAs in vivo, described in the pres-

ent manuscript, is under consideration for licensing from the authors' Institution (Max Planck Institute of Molecular Cell Biology and Genetics, Dresden, Germany) to a company, who may apply the described approach for potential future commercial applications. The authors will not receive any financial compensation or support for the experiments described in the present manuscript.

REFERENCES

1. Ruvkun, G.B. 2003. The tiny RNA world. *Harvey Lect.* 99:1-21.
2. He, L. and G.J. Hannon. 2004. MicroRNAs: small RNAs with a big role in gene regulation. *Nat. Rev. Genet.* 5:522-531.
3. Bartel, D.P. 2004. MicroRNAs: genomics, biogenesis, mechanism, and function. *Cell* 116:281-297.
4. Ambros, V. 2004. The functions of animal microRNAs. *Nature* 431:350-355.
5. Lagos-Quintana, M., R. Rauhut, A. Yalcin, J. Meyer, W. Lendeckel, and T. Tuschl. 2002. Identification of tissue-specific microRNAs from mouse. *Curr. Biol.* 12:735-739.
6. Krichevsky, A.M., K.S. King, C.P. Donahue, K. Khrapko, and K.S. Kosik. 2003. A microRNA array reveals extensive regulation of microRNAs during brain development. *RNA* 9:1274-1281.
7. Miska, E.A., E. Alvarez-Saavedra, M. Townsend, A. Yoshii, N. Sestan, P. Rakic, M. Constantine-Paton, and H.R. Horvitz. 2004. Microarray analysis of microRNA expression in the developing mammalian brain. *Genome Biol.* 5:R68.
8. Wienholds, E., W.P. Kloosterman, E. Miska, E. Alvarez-Saavedra, E. Berezikov, E. de Bruijn, H.R. Horvitz, S. Kauppinen, et al. 2005. MicroRNA expression in zebrafish embryonic development. *Science* 309:310-311.
9. Cheng, L.C., M. Tavazoie, and F. Doetsch. 2005. Stem cells: from epigenetics to microRNAs. *Neuron* 46:363-367.
10. Brennecke, J., D.R. Hipfner, A. Stark, R.B. Russell, and S.M. Cohen. 2003. bantam encodes a developmentally regulated microRNA that controls cell proliferation and regulates the proapoptotic gene *hid* in *Drosophila*. *Cell* 113:25-36.
11. Mansfield, J.H., B.D. Harfe, R. Nissen, J. Obenauer, J. Srineel, A. Chaudhuri, R. Farzan-Kashani, M. Zuker, et al. 2004. MicroRNA-responsive 'sensor' transgenes uncover Hox-like and other developmentally regulated patterns of vertebrate microRNA expression. *Nat. Genet.* 36:1079-1083.
12. Giraldez, A.J., R.M. Cinalli, M.E. Glasner, A.J. Enright, J.M. Thomson, S. Baskerville, S.M. Hammond, D.P. Bartel, et al. 2005. MicroRNAs regulate brain morphogenesis in zebrafish. *Science* 308:833-838.
13. Westerfield, M. 1993. The Zebrafish Book: A Guide for the Laboratory Use of Zebrafish *Danio (Brachydanio) rerio*. Institute of Neuroscience University of Oregon, Eugene, OR.
14. Takahashi, M., K. Sato, T. Nomura, and N. Osumi. 2002. Manipulating gene expressions by electroporation in the developing brain of mammalian embryos. *Differentiation* 70:155-162.
15. Calegari, F., W. Haubensack, D. Yang, W.B. Huttner, and F. Buchholz. 2002. Tissue-specific RNA interference in postimplantation mouse embryos with endoribonuclease-prepared short interfering RNA. *Proc. Natl. Acad. Sci. USA* 99:14236-14240.
16. Ingham, P.W. and H.R. Kim. 2005. Hedgehog signalling and the specification of muscle cell identity in the zebrafish embryo. *Exp. Cell Res.* 306:336-342.
17. Sempere, L.F., S. Freemantle, I. Pitha-Rowe, E. Moss, E. Dmitrovsky, and V. Ambros. 2004. Expression profiling of mammalian microRNAs uncovers a subset of brain-expressed microRNAs with possible roles in murine and human neuronal differentiation. *Genome Biol.* 5:R13.
18. Zhao, Y., E. Samal, and D. Srivastava. 2005. Serum response factor regulates a muscle-specific microRNA that targets *Hand2* during cardiogenesis. *Nature* 436:214-220.
19. Kloosterman, W.P., E. Wienholds, E. de Bruijn, S. Kauppinen, and R.H. Plasterk. 2006. In situ detection of miRNAs in animal embryos using LNA-modified oligonucleotide probes. *Nat. Methods* 3:27-29.
20. Smirnova, L., A. Grafe, A. Seiler, S. Schumacher, R. Nitsch, and F.G. Wolczyn. 2005. Regulation of miRNA expression during neural cell specification. *Eur. J. Neurosci.* 21:1469-1477.
21. Osumi, N. and T. Inoue. 2001. Gene transfer into cultured mammalian embryos by electroporation. *Methods* 24:35-42.

Received 23 February 2006; accepted 7 September 2006.

Address correspondence to Wieland B. Huttner, Max Planck Institute of Molecular Cell Biology and Genetics, Pfotenhauerstrasse 108, D-01307, Dresden, Germany. e-mail: huttner@mpi-cbg.de

To purchase reprints of this article, contact: Reprints@BioTechniques.com